

183

# SATELLITE & MESOMETEOROLOGY RESEARCH PROJECT

*Department of the Geophysical Sciences  
The University of Chicago*

## DIABATIC ANALYSIS

A NEW METHOD FOR PREDICTING TORNADO OUTBREAKS

by T. Theodore Fujita

Prepared for  
NASA/MSFC FY-80 Atmospheric Processes Research Review  
June 3-5, 1980 Huntsville, Alabama

SMRP Research Paper 183

June 1980

# DIABATIC ANALYSIS

A NEW METHOD FOR PREDICTING TORNADO OUTBREAKS

by

T. Theodore Fujita  
The University of Chicago

Prepared for

NASA/MSFC FY-80 Atmospheric Processes Research Review

June 3-5, 1980

Huntsville, Alabama

## A B S T R A C T

Basic equations of isentropic analysis were modified into those of diabatic analysis. Test analyses of tornado outbreak situations revealed that diabatic analysis is suitable in depicting both sinking and rising motions lasting 12 to 36 hours. It was found that a downslope wind occurs long before the development of an upslope wind in which mesocyclones form. Analysis works are on the way in an attempt to improve prediction of tornado outbreaks.

## 1. BASIC ELEMENTS OF TORNADO OUTBREAKS

It has been known that strong and violent tornadoes are spawned by rotating thunderstorms associated with mesocyclones. The basic elements of tornado outbreaks, therefore, are those which give rise to the formation of rotating thunderstorms.

Basic elements related to the formation of supercell, rotating thunderstorms are: --

- A. Upper-air Divergence ---- Significant divergence at the 200 to 300-mb jet-stream levels.
- B. Lower Convergence ---- Lateral convergence associated with low-level jet.
- C. Lifted Index ---- A measure of static instability of rising parcel.
- D. Low-level Moisture ---- High mixing ratio or dew-point temperature in the lowest 2,000 to 3,000 ft.
- E. Field of Rotation ---- Large absolute vorticity inside the inflow layer.

When these elements are amalgamated into a boiling pot, supercell tornadoes will pump low-level moisture up into the jet-stream levels. Huge rotating supercell storms, thus created, will spawn outbreak tornadoes. Figure 1 shows a flow diagram in which vorticity and instability are combined into the formation of rotating thunderstorms.

Constant-pressure charts, currently in use at most forecast offices, often show a significant PVA (positive vorticity advection) at 500 mb prior to a tornado outbreak. Meanwhile, an MAA (moist-air advection) intensifies in advance of a PVA.

In effect, the mid-level cooling and the low-level warming, along with the moisture influx, increase the INSTABILITY shown in Figure 1. ABSOLUTE VORTICITY at the low-level increases, because of the development of a surface low in advance of the PVA.

The processes of increasing both absolute vorticity and instability can also be explained by depicting the airflow on a potential temperature surface. Such a surface cuts through a number of constant-pressure surfaces. Both downslope and upslope winds can be described effectively on the surface with considerable slopes.

Analyses of a number of situations revealed that a pocket of down-slope wind is located near a significant PVA and that a tongue of up-slope wind, near an MAA.

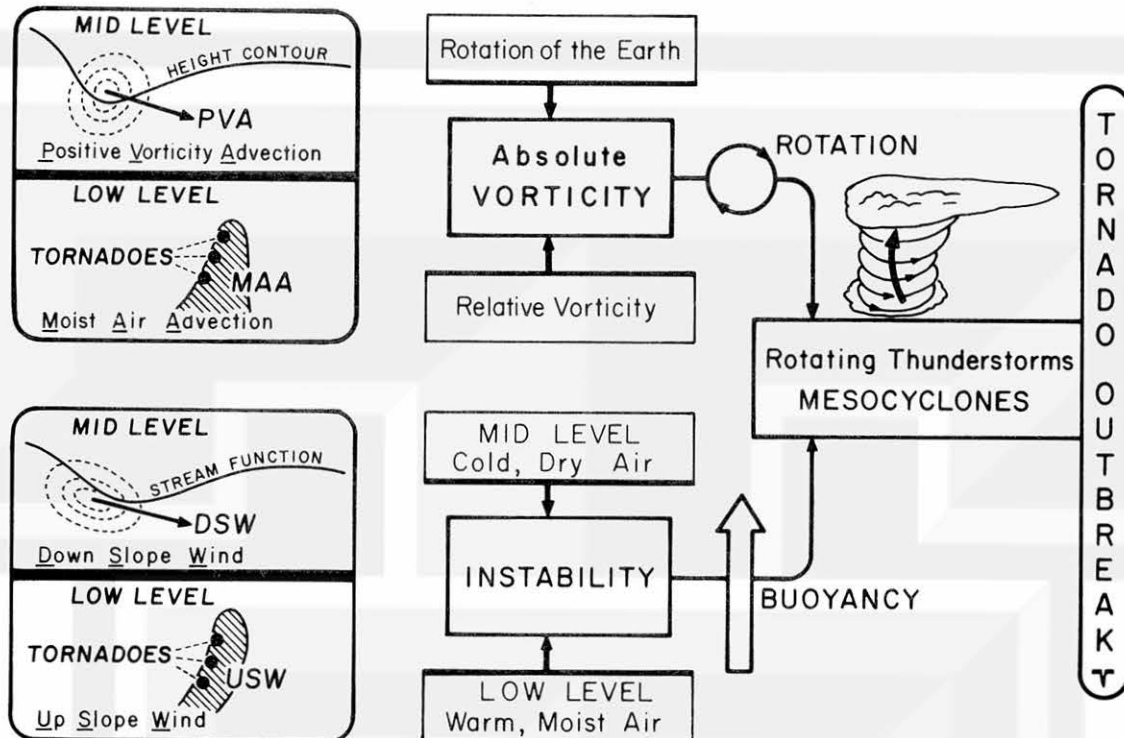


Figure 1. A flow diagram showing combined effects of INSTABILITY and VORTICITY which give rise to the formation and development of rotating thunderstorms. Rotating thunderstorms often identified as hook echoes, supercells, and mesocyclones spawn destructive tornadoes.

It has been found that a downslope wind (DSW) forms 24 to 36 hours prior to a tornado outbreak, while an upslope wind (USW) is induced 12 to 24 hours later. This encouraging evidence has led to a conclusion that the depiction of DSW and USW on a potential temperature surface is very useful in predicting tornado outbreaks with a 24- to 36-hour lead time.

## 2. ISENTROPIC AND DIABATIC PROCESSES

Isentropic analyses initiated notably by Rossby, et. al. (1937), Montgomery (1937), Byers (1938), and Namias (1938) were pursued by Oliver and Oliver (1951), Bjerknes (1951), Saucier (1955) and others. General interest in isentropic analysis, nonetheless, diminished during the late 1950s, because of time-consuming analyses with insignificant benefits to most forecasters.

A gradual comeback of isentropic analysis started in the mid to late 1970s, after about 20 years. Bleck (1975), Marks and Jones (1977), and Petersen (1979) demonstrated that objective analyses of isentropic charts can be achieved quickly and economically.

In requesting "Research Rapid Scan Days" for SMS GOES east and west satellites, the author was faced with the problem of predicting tornado outbreaks of Spring, 1980 24- to 36-hours in advance. For this purpose, a series of daily isentropic analyses was performed at the University of Chicago in March and April, 1980. These isentropic analyses led to the following findings: --

- A. An initial descending motion takes place at or above the 500-mb height.
- B. Taking 24 to 36 hours, the cold descending air reaches near the ground.
- C. The isentropic potential temperature decreases slightly during the slow descent, taking over a day.

It is very likely that the downslope wind does not warm up as much as the isentropic processes specify. Instead, the descending pocket of air is losing its internal energy through radiation, mixing, and other exchange processes.

Figure 2 shows schematically a diabatic descent of a downslope wind from 500 mb to the surface. If the descent is strictly adiabatic,  $-25^{\circ}\text{C}$  at 500 mb should warm up to  $0^{\circ}\text{C}$  at 700 mb, to  $+15^{\circ}\text{C}$  at 850 mb, and to  $+29^{\circ}\text{C}$  at 1000 mb. An upslope wind on the advancing side of the diabatic descent should also be diabatic -- or could be more diabatic due to the release of latent heat in clouds.

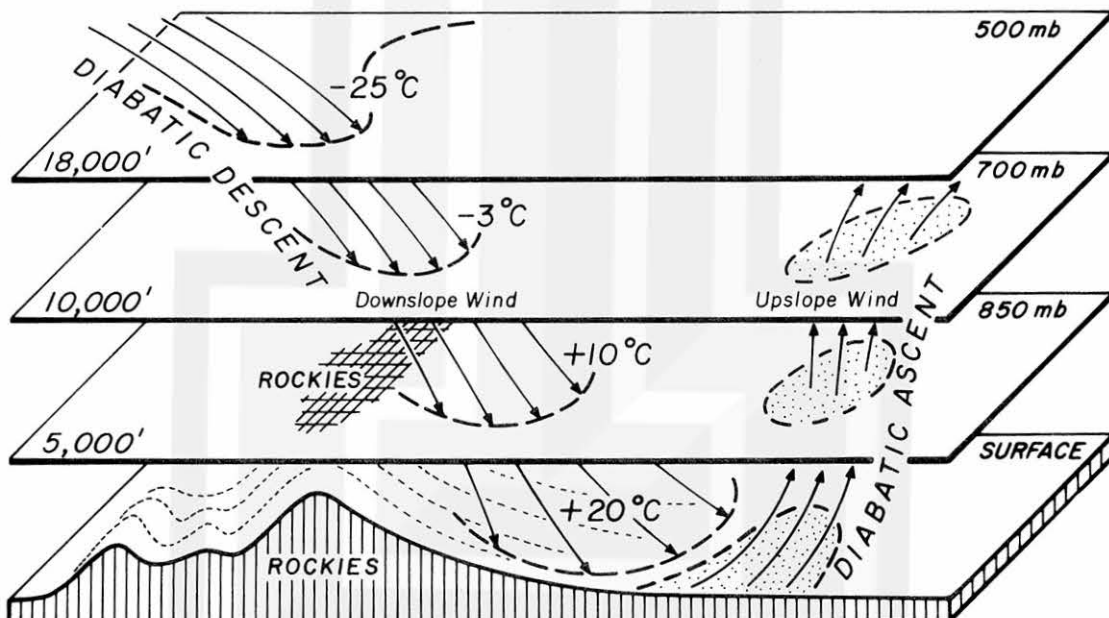


Figure 2. Schematic diagram of airflow undergoing the diabatic ascent induced by a diabatic descent. During diabatic processes, a descending parcel loses heat while an ascending parcel gains heat energy.

As a first step in formulating diabatic motions, taking one to two days, a following assumption has been made.

$$dQ = dU + dW \quad (1)$$

$$dQ = -\alpha dU \quad (\text{diabatic}) \quad (2)$$

where  $\alpha$  is a positive constant called the "diabatic constant". The diabatic constant is zero when the process is adiabatic.

The equations in Figure 3 show that this simplified diabatic process can be formulated by defining "diabatic potential temperature" which corresponds to "isentropic potential temperature".

$dQ = dU + dW$	
<u>ISENTROPIC</u>	<u>DIABATIC</u>
$0 = dU + dW$	$-\alpha dU = dU + dW$
$P T^{-\frac{C_p}{R}} = \text{Const.}$	$P T^{-\frac{C_p + \alpha C_v}{R}} = \text{Const.}$
<u>Isentropic Potential Temp.</u>	<u>Diabatic Potential Temp.</u>
$\theta = T \left( \frac{P}{1000} \right)^{\frac{R}{C_p}}$	$\phi = T \left( \frac{P}{1000} \right)^{\frac{R}{C_p + \alpha C_v}}$
<u>Isentropic Stream Function</u>	<u>Diabatic Stream Function</u>
$f V_g = \left( \frac{\partial \psi}{\partial n} \right)_\theta$	$f V_g = \left( \frac{\partial \zeta}{\partial n} \right)_\phi$
$\psi = C_p T + g H$	$\zeta = (C_p + \alpha C_v) T + g H$
$\Psi = \frac{\psi}{g} = (H + \frac{C_p}{g} T)$	$Z = \frac{\zeta}{g} = (H + \frac{C_p + \alpha C_v}{g} T)$

Figure 3. Basic equations of diabatic parameters obtained by the author early in 1980.

The Montgomery stream function is the special case of "diabatic stream function" which can be expressed by the function, Z, in meters. A diabatic chart will include

- \* Wind vector, ddf, on a specific diabatic potential temperature surface.
- \* Stream function, Z, which is contoured as if it were the height on a constant pressure chart. A contour interval of 30 or 60 m is preferable.
- \* Diabatic pressure, P, contoured in dashed lines like isotherms on a constant-pressure chart. Contour interval is 50 or 100 mb.

The following constants are used in computing diabatic equations in Figure 3.

$$R = 2.87 \times 10^6 \text{ erg g}^{-1} \text{ }^{\circ}\text{K}^{-1}$$

$$C_v = 5/2 R = 7.175 \times 10^6 \text{ erg g}^{-1} \text{ }^{\circ}\text{k}^{-1}$$

$$C_p = 7/2 R = 10.045 \times 10^6 \text{ erg g}^{-1} \text{ }^{\circ}\text{K}^{-1}$$

$$\frac{C_p + \alpha C_v}{R} = \frac{7 + 5\alpha}{2}$$

$$\frac{C_p + \alpha C_v}{g} = 102.6 + 73.2\alpha \text{ meter } ^{\circ}\text{K}^{-1}$$

Numerical values of diabatic potential temperature surfaces with -25°C temperature at 500 mb are presented in Tables 1 and 2.

Table 1. Temperature ( °C and °K) of isentropic and diabatic surfaces which intersect the 500-mb pressure height with -25°C isotherms.

	Mandatory Pressures					
	300	400	500	700	850	1000 mb
$\alpha = 0.0$	-58.7	-40.3	-25.0	0.0	+15.6	+29.3°C
	214.5	232.8	248.1	273.2	288.8	302.5°K
$\alpha = 0.1$	-56.6	-39.4	-25.0	-1.7	+12.7	+25.3°C
	216.5	233.8	248.1	271.4	285.8	298.5°K
$\alpha = 0.2$	-54.8	-38.5	-25.0	-3.2	+10.2	+21.9°C
	218.4	234.7	248.1	269.9	283.4	295.1°K

Table 2. Values of  $\Psi - H$  and  $Z - H$  for mandatory pressure heights. Isentropic and diabatic stream function can be obtained by adding the height of the isentropic surface to the numbers in this table. (Unit in 10 meters)

	Mandatory Pressures					
	300	400	500	700	850	1000 mb
$\alpha = 0.0$	2201	2389	2546	2803	2963	$3104 \times 10$ m
$\alpha = 0.1$	2380	2570	2727	2983	3141	$3281 \times 10$ m
$\alpha = 0.2$	2560	2752	2909	3164	3322	$3460 \times 10$ m

### 3. ENERGY CASCADE

Diabatic analysis of tornado outbreak situations revealed a cascade of energy from the general circulation-scale down to the tornado scale. Evidently, the downslope wind plays a key role in accomplishing the cascade of energy (see Figure 4).

The initial formation of a downslope wind takes place to the west or northwest of the Rockies at 300- to 500-mb heights, 12 to 24 hours prior to the onset of the upslope wind. At this point, the cause and effect relationship between upslope and downslope winds is evident; a downslope wind, which originates first, induces an upslope wind.

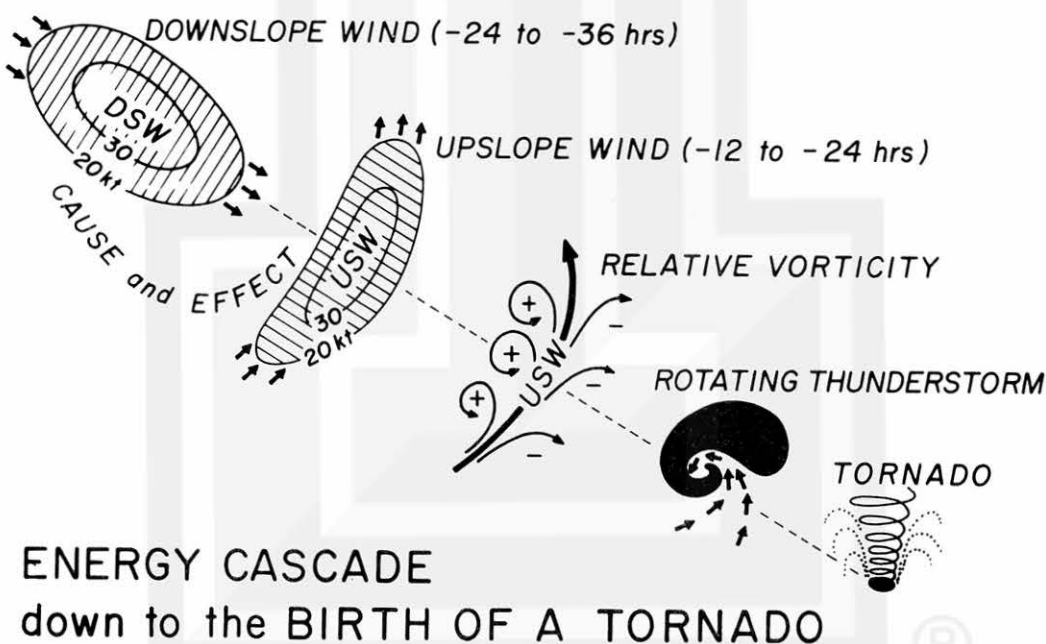


Figure 4. Energy cascade from downslope wind, rotating thunderstorm, finally to tornado.

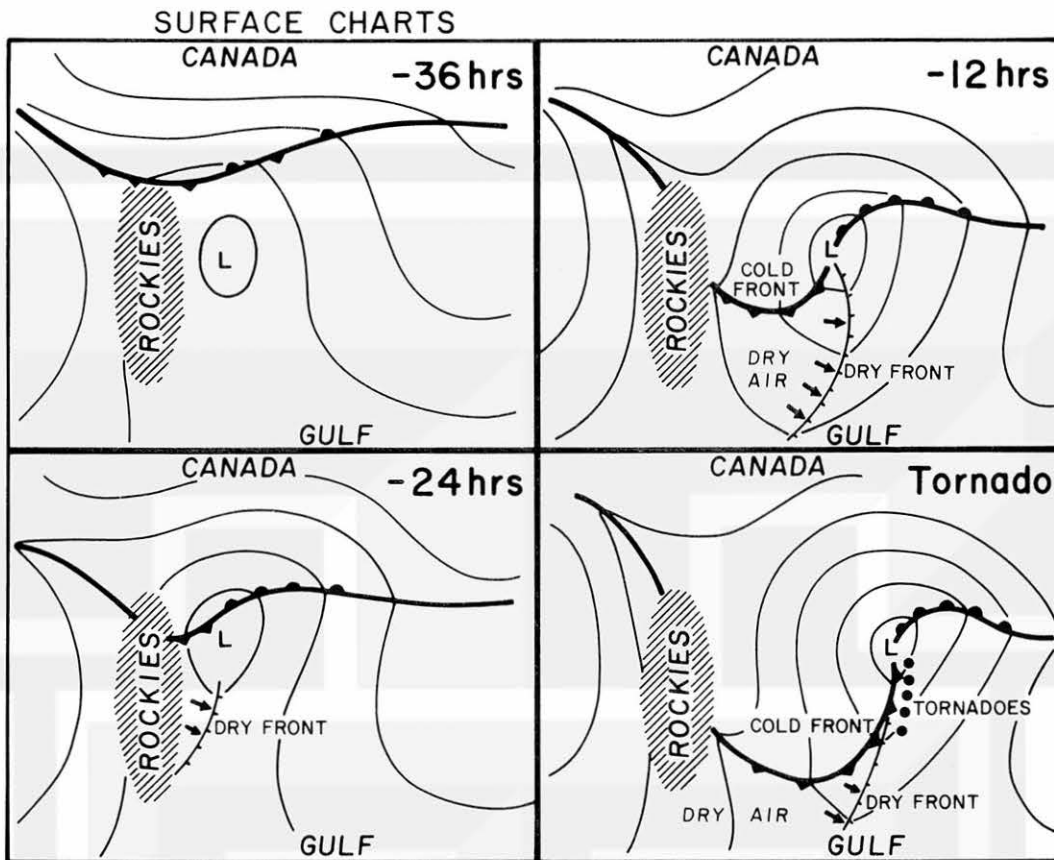


Figure 5. Four surface charts at 12-hour intervals prior to an outbreak of tornadoes. Tornadoes often form ahead of cold front.

$295.1^{\circ}\text{K}$   $\alpha = 0.2$  DIABATIC CHARTS

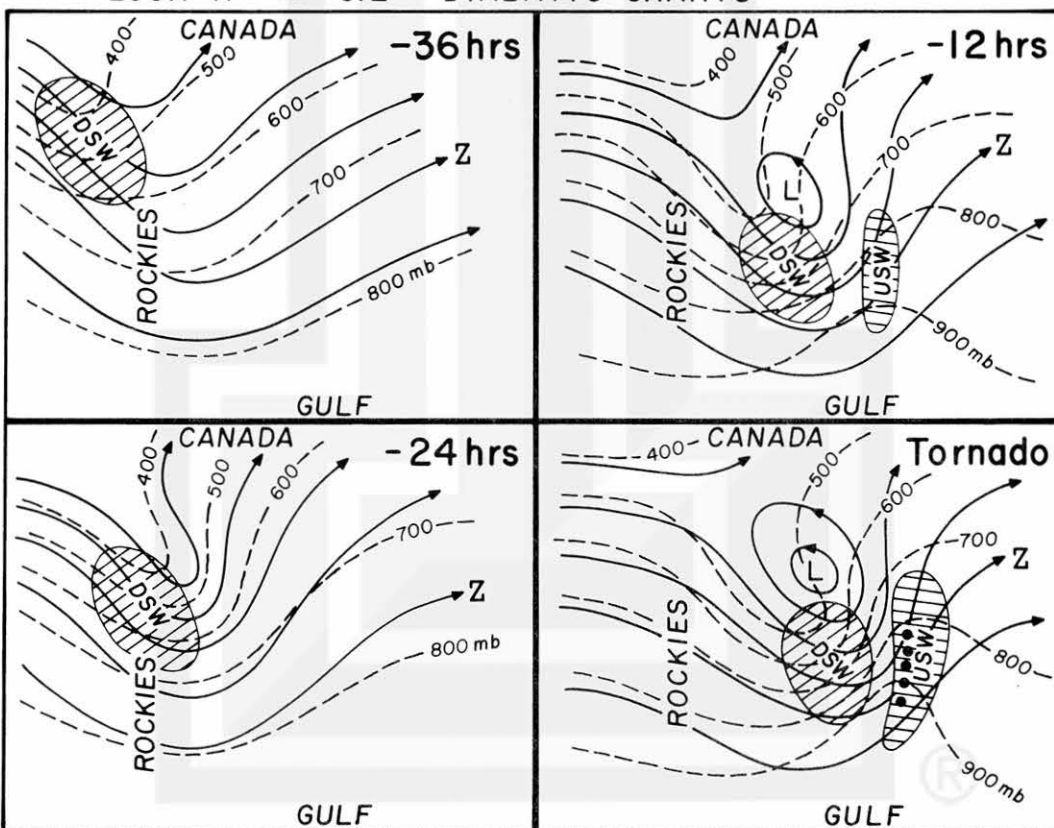


Figure 6. Four diabatic charts at 12-hour intervals corresponding to the surface charts in Figure 5. These charts show that a down-slope wind from the northwest is an excellent predictor.

Apparently, the downslope wind, during its long-distance descent, generates positive vorticity on the left (northeast) side. By the time the downslope wind reaches the low level, a significant vorticity field appears at all levels. Thus, a PVA takes place in the immediate area of the downslope wind.

The transformation of energy leading to the development of upslope wind is achieved by the downslope wind which descends with its large momentum brought down from its initial altitude. The downslope wind, in effect, contributes to the cyclogenesis throughout the entire depth of the troposphere.

A significant upslope wind results in warm advection at low levels. Meanwhile, the field of intense vorticity on the left side of the upslope wind provides thunderstorms with cyclonic circulations required to develop these storms into rotating thunderstorms, supercells, mesocyclones, or hook echoes. It has been known that rotating thunderstorms, during their lives, are the mother clouds that spawn strong and violent tornadoes.

A time sequence of the event which leads to a tornado outbreak is presented in Figures 5 (surface chart) and 6 (diabatic chart). The surface charts imply that an outbreak of tornadoes occurs along the leading edge of the cold air from Canada as it pushes violently eastward.

Diabatic charts, on the other hand, depict an area of downslope wind heading toward the Rockies some 24 to 36 hours in advance of a tornado outbreak. As the downslope wind passes over the Rockies, cyclogenesis takes place on the east side of the Rockies.

It should be noted that the upslope wind at -12 hrs is located on the advancing side of the downslope wind which is dry and quite often warmer than the warm, moist air on or near the ground. The cold front of Canadian air is located far behind the dry front which signifies the leading edge of the downslope wind.

The cold front may or may not overtake the dry front prior to the onset of a tornado outbreak. If it does, a line of tornadoes will develop along the cold front; if it does not, a tornado outbreak occurs way ahead of the cold front.

#### 4. EFFECT OF TIBET UPON TORNADOES IN CHINA

A series of diabatic charts analysed by the author seems to indicate that the cold front located in the vicinity of a tornado outbreak is of secondary importance upon its outbreak. In other words, an active cold front may not be required in order to set off an outbreak. Instead, a significant downslope wind and associated upslope wind seem to play an important role upon the onset.

Surface and upper-air charts over China were analysed for testing this hypothesis. Tornadoes are known to be rare and weak in China while cold fronts are strong and frequent there.

The topographic environment of east-central China is similar to that of the United States Midwest. There are high mountains to the west and warm tropical waters to the south.

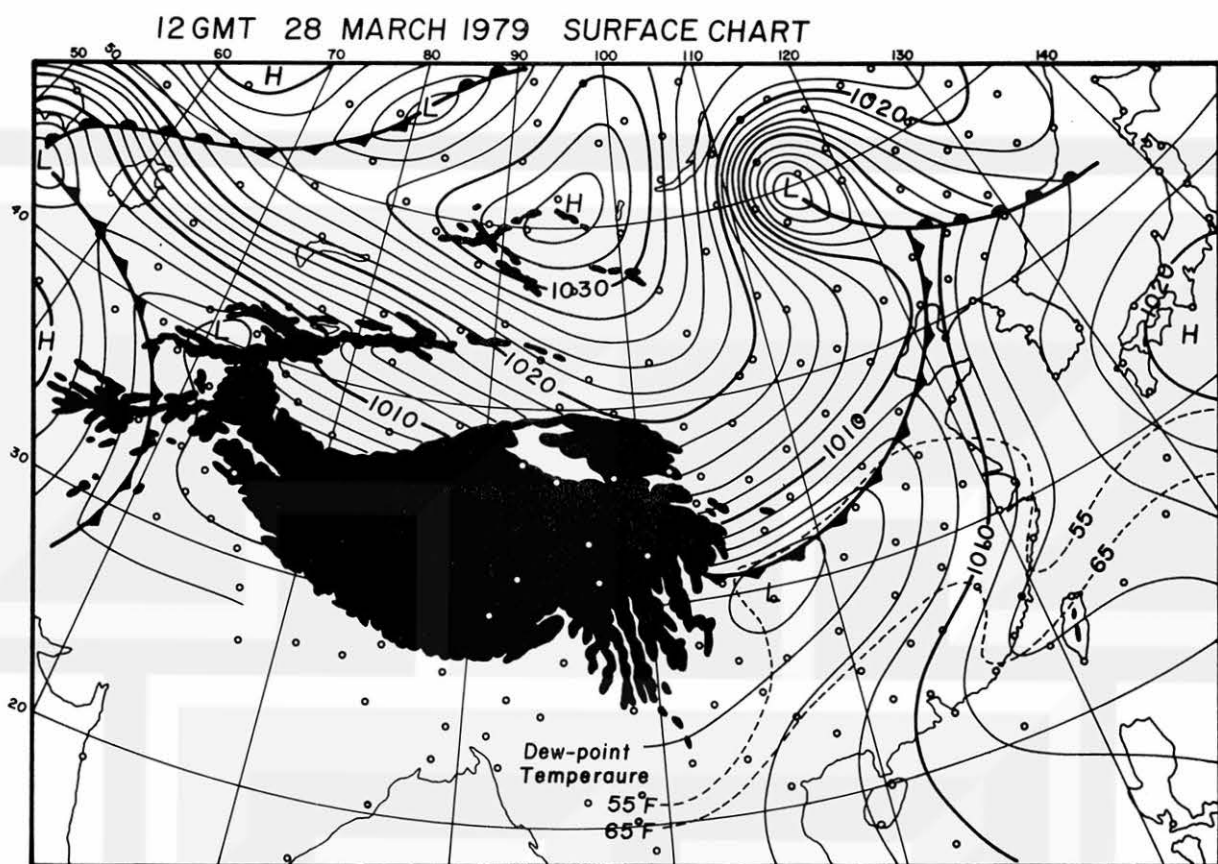


Figure 7. A cold front over China.

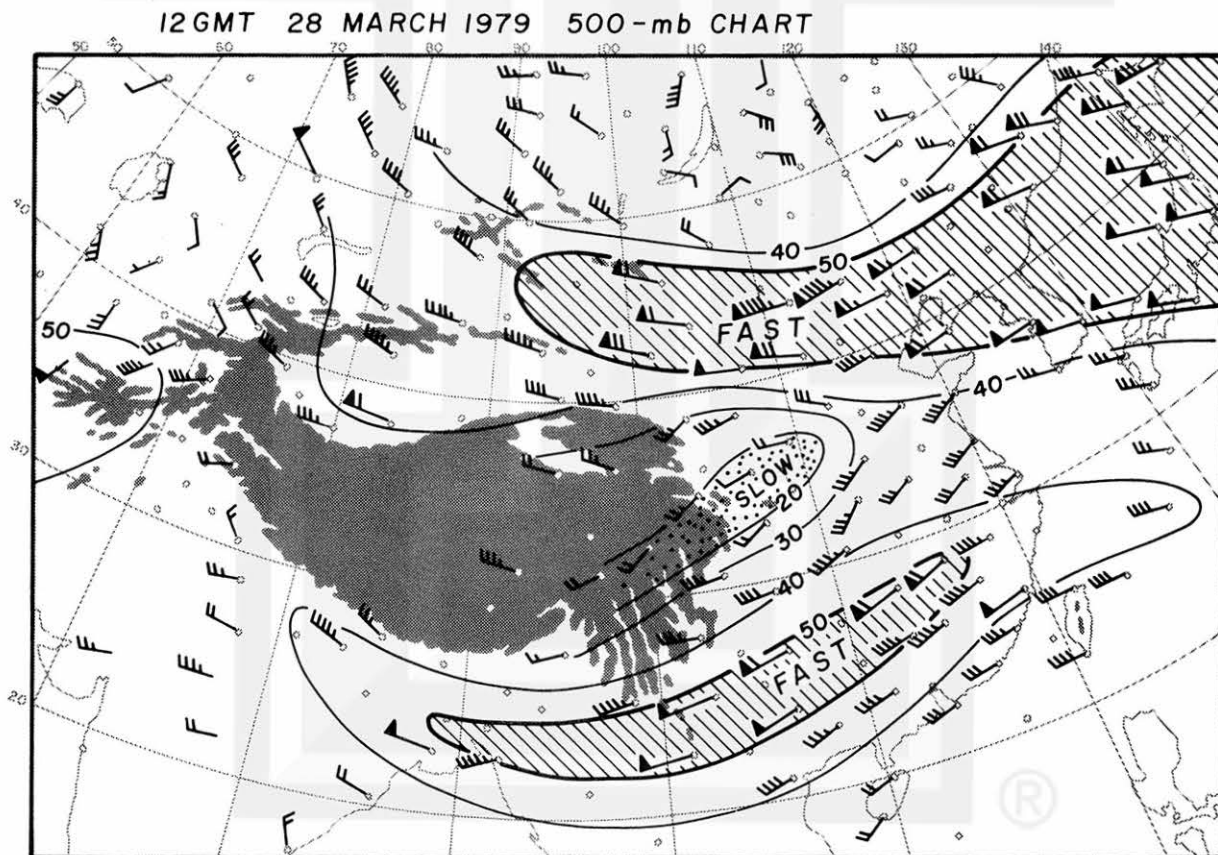


Figure 8. Split of westerlies caused by the highland of Tibet.

Figure 7 is a surface chart at 12 GMT on March 28, 1979, showing an example of a well-developed cold front extending from the Yellow Sea to the eastern edge of Tibet. If a frontal situation similar to this chart prevails over the United States in Spring, a number of damaging tornadoes are expected to occur, resulting in a few tornado watch boxes. In China, however, tornado outbreaks are rare or nonexistent. What is the major difference in synoptic situations?

Figure 8 shows a 500-mb chart which corresponds to the surface map of Figure 7. As seen clearly in this chart, the highland of Tibet splits the westerlies into northern and southern streams. The southern stream with up to 60 kt wind extends from northern India to Okinawa, while the northern stream extends from Gobi to the Sea of Japan.

In the downstream of Tibet, between the northern and southern streams, there is a weak, stagnation flow with winds up to only 20 kt at 500 mb. As expected, a more significant stagnation and split flow is seen at 700 mb. It is very likely that a combination of orographic and thermal effects of Tibet alters the upper-air flow over eastern China completely.

Apparently, Tibet is much higher and larger than the Rockies. Proper-sized mountains, such as the Rockies, do enhance tornado activities. The highland of Tibet, on the other hand, splits the westerly flow into two, thus eliminating the possibility of a significant downslope wind entering into the east China plain from the west or northwest. If mountains are too high and extensive, their presence suppress tornado activities. It would be useful to investigate the possible effects of Tibet upon weather and climate of eastern China and western Japan.

The unique feature of Tibet is its large body of relatively flat plateau attached to the Pamirs, something like a tail extending westward. The Pamirs, known as the roof of the world, is connected to folded mountains with a large number of roughness fins sticking out toward the northwest. These fins are likely to reduce the flow speed of the north branch of the split flow (see Figure 7).

Speculative Drawings of Jupiter's Red Spot with Tibet-like Mountain underneath

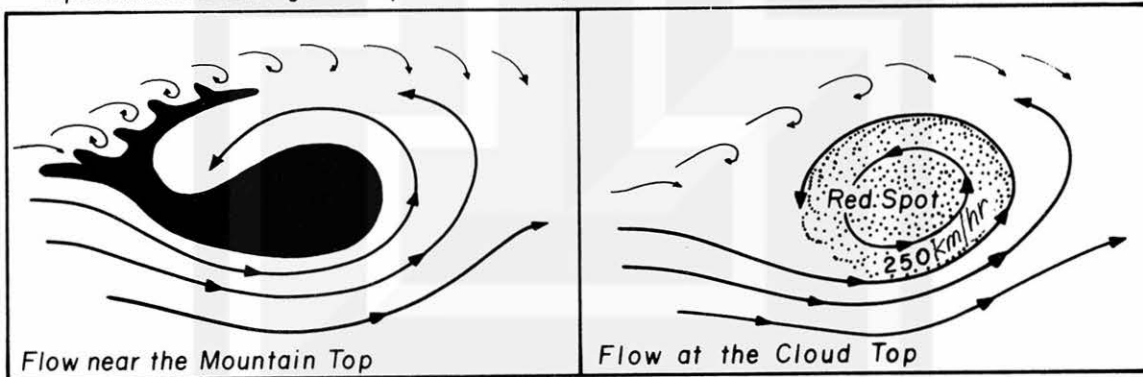


Figure 9. Is there Tibet-like highland beneath Jupiter's Red Spot, a giant swirl of 250 to 280 km/hr.

If the southern edge of the Himalayas was polished smooth, the south branch of the split flow will be accelerated by the Bernoulli effect without friction. The cyclonic flow, thus generated, could circle around the east edge of Tibet inducing a large cyclone.

The purpose of speculating on a possible mechanism of Jupiter's Red Spot is to emphasize the effect of a super-mountain/plateau, such as Tibet, upon an impinging current (see Figure 9).

## 5. DIABATIC ANALYSIS OF SESAME-79 DATA

AVE-SESAME sounding data on April 10, 1979, the day of the Wichita Falls tornado, were analysed in detail. Presented herewith are examples of diabatic analyses with 295 °K potential temperature.

Figure 10 was prepared to show a downslope wind, in excess of 30 kt, descending over California heading toward New Mexico. An upslope wind began intensifying over southeastern Texas. Time: 6 a.m. April 10, 1979, some 12 hours before the Wichita Falls tornado.

Three hours before the tornado (see Figure 11), the downslope wind reached over the Arizona-New Mexico border. Upslope wind moved up with its axis extending from the Red River valley to near Omaha, Nebraska. A couple of tornadoes occurred on the left (cyclonic) side of the upslope-wind axis.

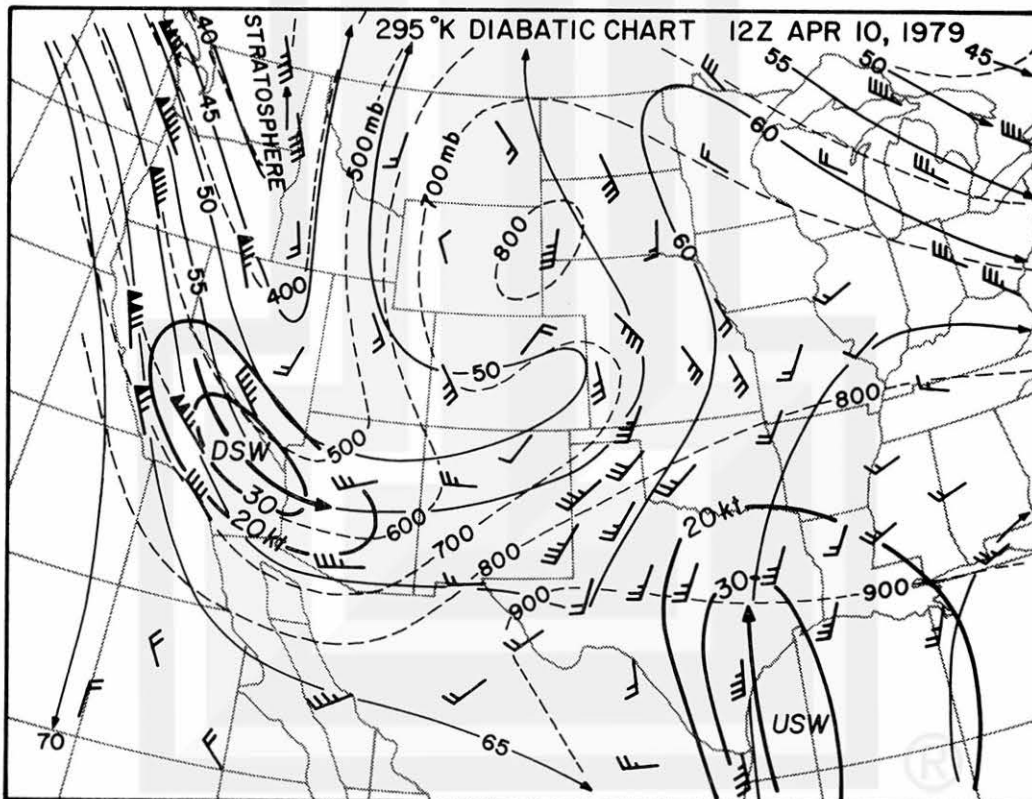


Figure 10. Diabatic chart 12 hours before the Wichita Falls tornado.

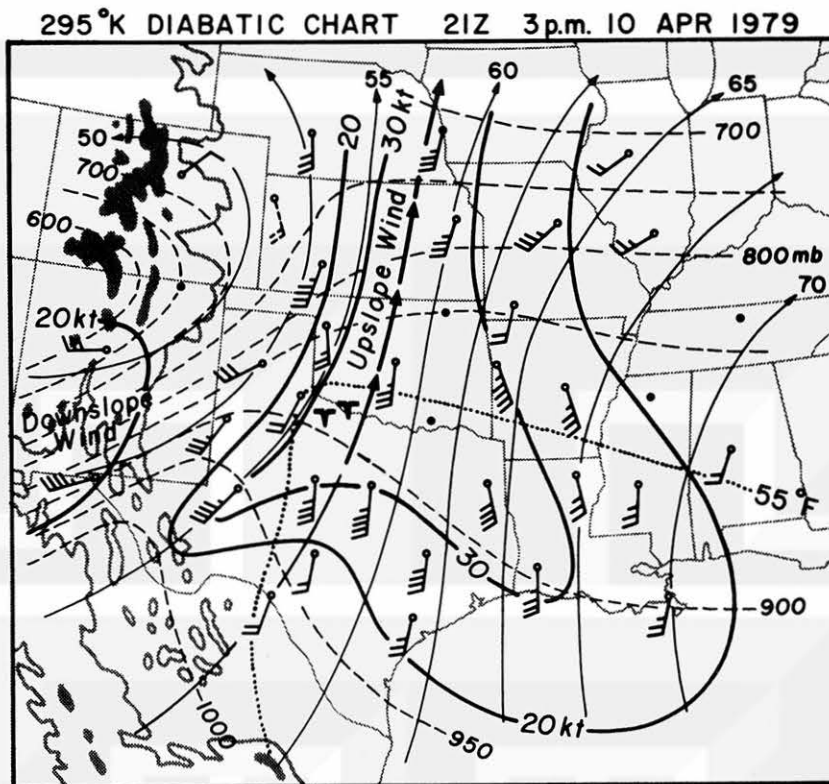


Figure 11. Local diabatic chart 3 hours before the tornado.

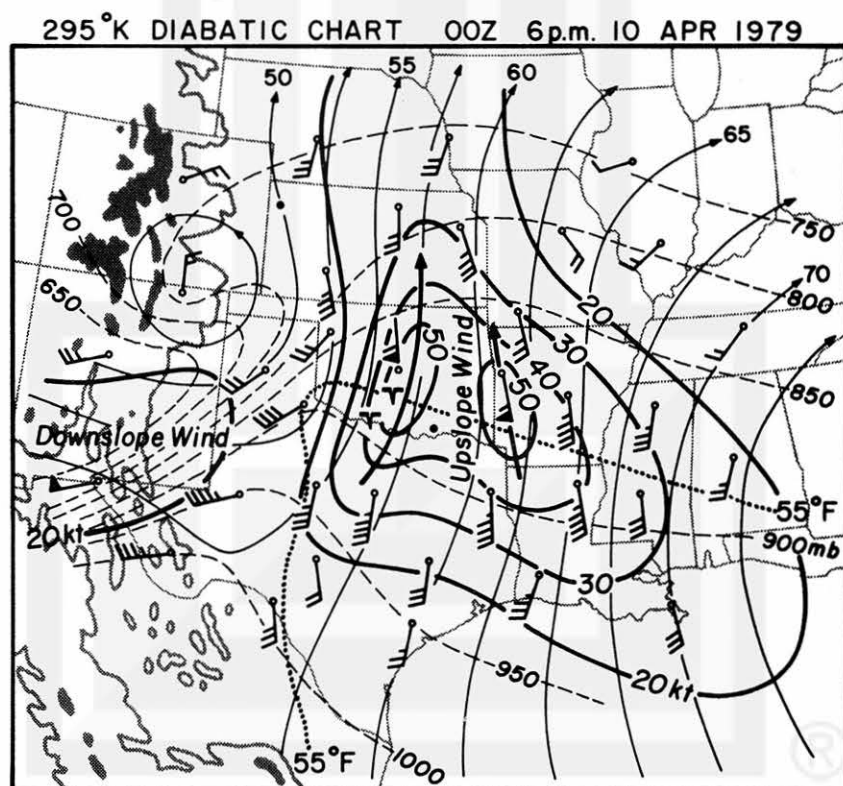


Figure 12. Local diabatic chart at the time of the tornado.

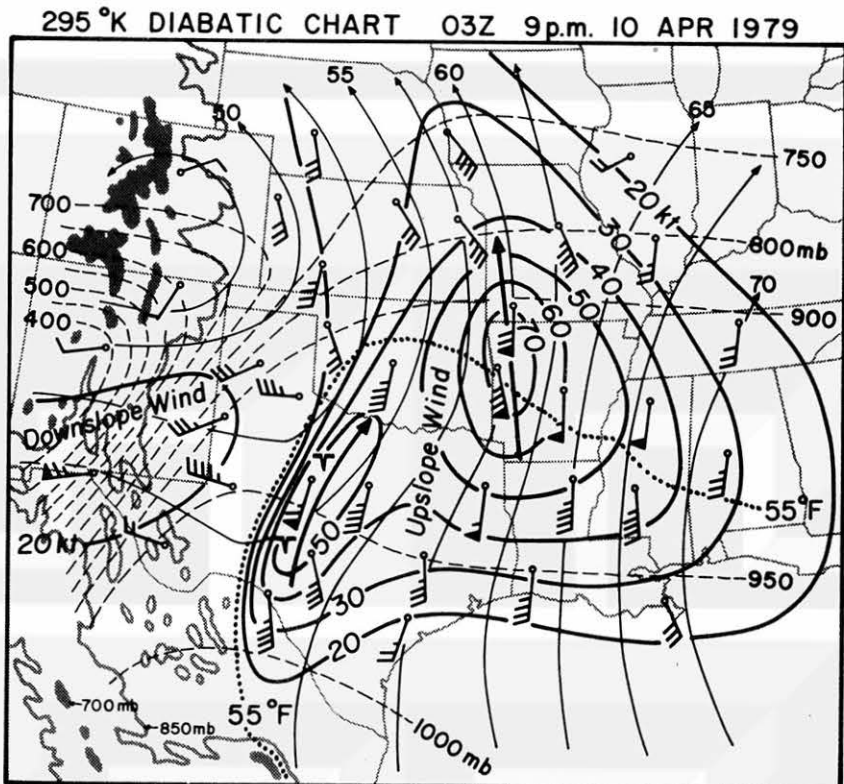


Figure 13. Local diabatic chart 3 hours after the tornado.

When the Wichita Falls tornado occurred at about 6 p.m. (see Figure 12), the downslope wind over New Mexico was strong. The tornado occurred on the left (cyclonic) side of the upslope-wind axis.

Three hours after the Wichita Falls tornado, a new upslope wind developed on the advancing side of the downslope wind. Weak night-time tornadoes were reported in central Texas.

## 6. CONCLUSIONS

The diabatic analysis presented in this paper is designed to be identical, in procedures, to isentropic analysis familiar to meteorologists for the last five decades. Vertical velocities of both isentropic and diabatic flows cannot be computed without subtracting the isobar movement. Nonetheless, steeper slope of the diabatic surface, in comparison with isentropic surface, allows us to depict upslope and downslope winds effectively.

It is recommended that this proposed diabatic analysis be tested further in order to improve early prediction of tornado outbreaks. Specific recommendations are: --

- A. To carry out AVE experiments over the western parts of the United States to investigate the nature of downslope wind, a new predictor of tornado outbreaks.

- B. To develop Severe-Storm and Mesoscale Environmental Research Satellite (SMEARS) with improved sounding capabilities in the presence of high clouds. Such a satellite is extremely useful in detecting and tracking a downslope wind from the northeastern Pacific to the immediate vicinity of tornado areas.
- C. To pursue diabatic analyses over the other parts of the world to determine the influence of giant mountains. The highland of Tibet appears to be the best orography to be studied.
- D. To conduct global analyses of diabatic charts in describing three-dimensional motions of the global atmosphere.

#### ACKNOWLEDGEMENT:

The research work presented in this paper has been sponsored by NASA, NGR 14-001-008 and NOAA, under NA80AA-D-00001.

#### R E F E R E N C E S

- Bjeknes, J. (1951) Extratropical cyclones. Comp. of Meteorology, AMS. 577-598
- Bleck, R. (1975) An economical approach to the use of wind data in the optimum interpolation of geo- and Montgomery potential fields. Mon. Wea. Rev. 103, 807-816
- Byers, H. R. (1938) On the thermodynamic interpretation of isentropic charts Mon. Wea. Rev. 16 3
- Marks, D. G. and R. V. Jones (1977) An operational analysis scheme on isentropic surfaces. Preprints of A.M.S. Conf. on N.W.P.
- Montgomery, R. B. (1937) A suggested method for representing gradient flow in isentropic surfaces. Bull. of A.M.S. 18, 6-7
- Namias, J. (1938) Thunderstorm forecasting with the aid of isentropic charts. Bull. of M.S. 19 1
- Oliver, V. J. and M.B. Oliver (1951) Meteorological analysis in the middle latitudes. Comp. of Meteorology, A.M.S. 715-726
- Petersen, R. A. (1979) Three-dimensional objective analysis using an isentropic cross-sectional technique. Preprint of 11th Conf. on Severe Local Storms. 20-27
- Rossby C.-G. et Al. (1937) Isentropic Analysis. Bull. of A.M.S. 18 201-209
- Saucier, W. J. (1955) Principles of Meteorological Analysis. University of Chicago Press. 438 pp